Machine Copy for Proofreading, Vol. x, y–z, 2011

ELECTROMAGNETIC DESIGN OF A MAGNETIC FIELD SOURCE FOR A MAGNETOCALORIC REFRIGERATOR

H. R. E. H. Bouchekara[1,*], A. Kedous-Lebouc[2], and J. P. Yonnet[2]

[1]Department of Electrical Engineering, College of Engineering and Islamic Architecture, Umm Al-Qura University, P. O. Box 5555, Makkah 21955, Saudi Arabia

[2]Grenoble Electrical Engineering Laboratory, Grenoble-INP, UJF Grenoble 1, CNRS UMR 5269, G2Elab, Bat. ENSE3, BP 46, Saint Martin, d'Hères Cedex 38402, France

Abstract—In this paper, several configurations of a rotary magnetic refrigerator are proposed and investigated using three dimensional finite element method simulations. Their electromagnetic performance is analyzed considering the magnetic flux density, the forces and the torque. The rotor is a single permanent magnet while the stator is made of four refrigerant beds and a magnetic yoke. Multipole stators or rotors with 4, 6 and 8 refrigerant beds have been tested. The beds can be fitted or set at the inner surface of the yoke. The yoke can have smooth or salient poles. To minimize the magnetic torque, an original structure is proposed and tested. It is composed of two half-systems assembled with a 45° angle shift between rotors or stators. Because of the large amount of data, a suitable procedure to achieve an effective comparison between all configurations is established.

1. INTRODUCTION

The future of magnetic refrigeration looks bright. Much research is ongoing in the field of magnetocaloric materials and magnetic refrigeration systems to find a suitable way to make an efficient machine [1–3]. Even though significant advances are achieved in giant magnetocaloric materials around room temperature and the feasibility

Received 27 June 2011.
* Corresponding author: Houssem Rafik El Hana Bouchekara (bouchekara.houssem@gmail.com).

of magnetic cooling technology has been demonstrated through several prototypes [4–6], more work on both the fundamental and practical plane is needed to master this technology and introduce it in industrial and domestic applications [7–11].

Magnetic refrigeration (MR) is based on the magnetocaloric effect (MCE); defined as an intrinsic property of some magnetic materials which respond to an external applied magnetic field by a variation in their temperature. The temperature increases when the magnetic field is applied (magnetization phase) and decreases when the magnetic field is removed (demagnetization phase). This shows the fundamental and important role of the applied magnetic field. Thus, the design of the magnetic field source in MR systems should be one of the first issues that researchers should focus on. On the international level, many teams are working on new MR systems structures [3]. Particular efforts have been done to increase magnetic induction for more powerful MR systems [12–17].

The operation and performance of magnetic cooling system are governed by many factors closely interacting with each other. This paper presents the design of a rotating multipole magnetic field source using finite element simulations. To optimize the performance of such a system, several configurations are proposed. The performances of all configurations are compared to each other according to three major criteria: magnetic induction level, forces and torque (magnetic efforts).

We report the electromagnetic computations performed with the commercial finite element software namely, Flux® [18]. Computations are undertaken to maximize the magnetization in order to get the best MR performance (temperature span and cooling power) and limit mechanical efforts (forces and torque).

2. STUDIED CONFIGURATIONS

2.1. Description of the Initial Configuration

The initial rotating machine configuration called Structure ⓪, is the one used in our magnetic refrigeration prototype [16, 19, 20]. It is similar to some existing prototypes [9, 14]. The rotor is a permanent magnet and the stator is made of a magnetic yoke and four refrigerant beds named in a clockwise order b_1, b_2, b_3 and, b_4 (Fig. 1(a)).The yoke is composed of four poles to concentrate the magnetic flux within the four refrigerant beds. The magnetization and demagnetization phases are obtained by a simple rotation of the permanent magnet. The beds undergo an active magnetic regenerative refrigeration cycle (AMRR) and operate two by two in the opposite way, i.e., if b_1 and b_3 are magnetized b_2 and b_4 are demagnetized and vice versa. This working

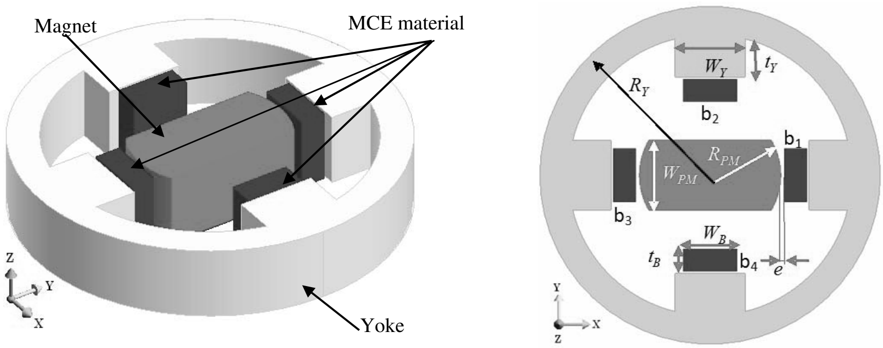

(a) (b)

Figure 1. Structure ⓪ configuration and main dimensional characteristics.

Table 1. The main geometrical parameters.

Name	Description	Value
R_{PM}	magnet radius	53.5 mm
W_{PM}	magnet width	53.0 mm
R_Y	yoke external radius	129.0 mm
t_Y	yoke pole thickness	29.0 mm
W_Y	yoke pole width	53.0 mm
W_B	Bed width	40.0 mm
t_B	Bed thickness	17.0 mm
e	Airgap bed/magnet	1.70 mm

principle allows increasing the output cooling power of the system. The main geometrical parameters are defined in Fig. 1(b) and their values are given in Table 1.

2.2. Description of the Different Studied Configurations

Structure ⓪ is optimized to provide the highest induction level in the given volume of MCE material. It is chosen because of its easy construction. However it induces high mechanical stresses on both the refrigerant beds and the driving actuator. More poles are better to minimize the magnetic torque but it leads to a more complex AMRR cycle. A first, quick, and original solution was found to overcome the torque issue. This solution uses a passive torque compensation system which is an 8 poles synchronous magnetic coupling, designed to produce the same torque as the MR prototype [19] but with opposite phase. With this solution a reduction of 10 was achieved.

Alternatively, a complete study was performed to improve the Structure ⓪ [19], and as a result eight new configurations were proposed and their magnetic behaviors were studied. For all configurations, the sizes of the magnet, the refrigerant bed and the airgap are fixed. Then, the stator structure is modified to study the influence of the number of beds, the yoke shape, etc.. These structures are presented in Fig. 2 and they can be briefly described as follows:

- Structure ① is nearly the same as the initial one. Only the refrigerant beds and the stator poles have been modified from rectangular to cylindrical shapes (the same as the rotor shape) as shown in Fig. 2(a).
- Structure ② has the same shape of the initial configuration. Nonetheless, the number of MCE material blocks is increased to study its influence on the magnetic behavior of the magnetic field source. Increasing this number theoretically decreases the magnetic torque of the system. So a 6-pole yoke and 6 refrigerant beds are used instead of 4. All the other parts and dimensions are kept identical (Fig. 2(b)).
- Structure ③ has the same shape and the same number of refrigerant blocks as Structure ⓪. However, Structure ③ has a smooth yoke without any pole (Fig. 2(c)). The objective of this structure is to study the influence of the yoke poles.
- Structure ④ is similar to Structure ③ but has 6 blocks instead of 4 (Fig. 2(d)). The aim of this structure is to study the influence of the number of MCE material blocks in a structure without yoke poles.
- In Structure ⑤, another solution to reduce the magnetic torque is investigated. The initial structure is split into two-half structures which are assembled in such a way to compensate their torques. This can be achieved by a 45° angle shift of either one of the stators or the rotors as shown in Fig. 2(e) for Structure ⑤-a and Structure ⑤-b, respectively. In both structures the distance between the two parts should be optimized in order to reduce their interactions. In our case this distance is found equal to the half the length of the structure. This configuration is very interesting; it allows obtaining multi-stage structures. This will increase the power cooling of such systems.
- In Structure ⑥, the 4 refrigerant beds are inserted into the yoke as shown in Fig. 2(f). In this case, the yoke is larger than the

initial structure. Its role is to canalize the magnetic flux as well as to maintain mechanically the beds.

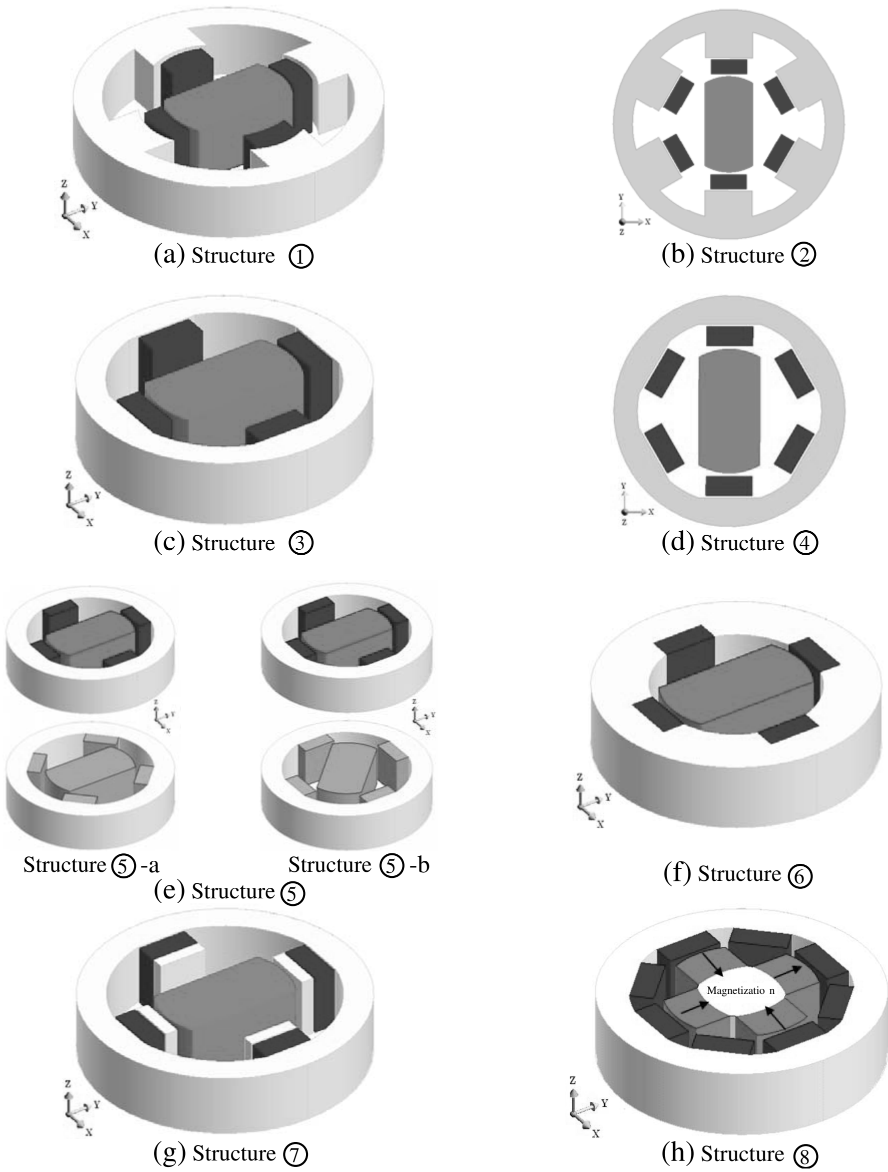

Figure 2. Description of the 8 configurations derived from structure ⓪.

- Structure ⑦ is similar to Structure ③, but wedges are set on the beds in front of the magnet (Fig. 2(g)). They are additional 10 mm thick steel parts aimed to support the tangential forces instead of the materials beds.
- The Structure ⑧, has four poles at the rotor, eight refrigerant beds and a smooth poles yoke at the stator (Fig. 2(h)).

In addition to these 8 structures, some other combinations are possible among the proposed ones, for instance the number of blocks can be increased to 8 with cylindrical or rectangular shapes.

2.3. Finite Element Simulation Conditions and Analysis Criteria

The finite element simulations were performed using FLUX® software in three dimensions. An infinite box is used to take into account the end effects. To save numerical cost and memory, the length of the structure is fixed to 50 mm. This induces higher 3D effects than in the real structure which is three times longer. The problem has been solved in magnetostatic formulation. Rotor motion is easily taken into consideration thanks to its position parameterization.

In all the studies, the remanent magnetization and the relative permeability of the magnet are fixed respectively to 1.47 T and 1.067 (NdFeB magnets). The stator is described by the non linear B(H) law of XC10 steel and the MCE material by an isotropic bulk gadolinium material with a relative permeability of 2 (Fig. 3). No eddy current or hysteresis is considered.

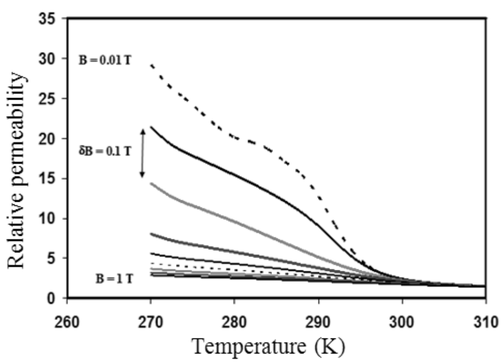

Figure 3. The relative permeability of the gadolinium versus the temperature and function of the magnetic induction.

Because of the large number of simulations, a numerical tool has been developed to compare the different structures in an effective way. It makes a link between MATLAB® and FLUX® softwares. It allows defining the simulation conditions, starting the resolutions, and computing the desired quantities from the results obtained by Flux. Thus, the following magnetic quantities are scanned as a function of the rotor position:

- magnetic induction evolution against θ in different points of a grid defined in the four beds
- maximum, minimum, and average $B(\theta)$ values
- magnetic torque supported by each part of the structure magnetic forces undergone by the refrigerant beds.

3. RESULTS AND DISCUSSION

Figure 4 gives the main results obtained with Structure ⓪. For $\theta = 0$, the magnet is set along the Y axis. The two beds (b_1, b_3) are magnetized while (b_2, b_4) are demagnetized, the induction level in the centre of each bed varying from 0.05 to 0.94 T. The computation in different points of the material showed that the average bed induction is almost the same as its average value taken in the bed centre. The difference observed is about 5%. The total torque of the structure is the cogging torque computed on the rotor. It has also the opposite value of the torque obtained on the stator. It varies sinusoidally with the magnet position and its maximum value is about 20 Nm. The magnetic forces components F_X and F_Y vary differently with the angle position θ. Their maximum values are respectively about 80 N and 95 N. These torque and forces are quite high and seriously impact the mechanical withstand of the bed frame and also the fluid flow [20].

These results suggest the following comments:

- As pointed out before, Structure ⓪ allows the highest possible induction level. In addition, $B(\theta)$ evolution is the most trapezoidal one. This ensures a better magnetization and demagnetization cycle. As a negative consequence, the cogging torque and forces are very high.
- A smooth yoke decreases the total torque. In that case, the reluctance variation is only due to MCE magnetic beds which act as additional poles. The maximum induction level is a little bit lower and forces are almost the same. The reduction of the torque is more important in the case of four refrigerant beds Structures (⓪ to ③). For Structures ② and ④, the torque is mainly due

to the refrigerant beds geometry and the yoke shape influence is negligible.

- Increasing the number of beds from 4 to 6 strongly decreases the magnetic torque for both salient and smooth pole yoke structures (by comparing Structure ⓪ to ② and Structure ③ to ④, reduction factors of 5 and 4, respectively are achieved). However the interactions between the beds are stronger and lead to both a decrease of the induction level, and a smoother magnetic field excitation.
- Torque cancellation is almost achieved in the Structure ⑤ due to the cascade arrangement. The induction and force variations are not modified. A system with several shifted blocks can be considered to increase the cooling power or investigate different MCE materials in order to enlarge their temperature working range.

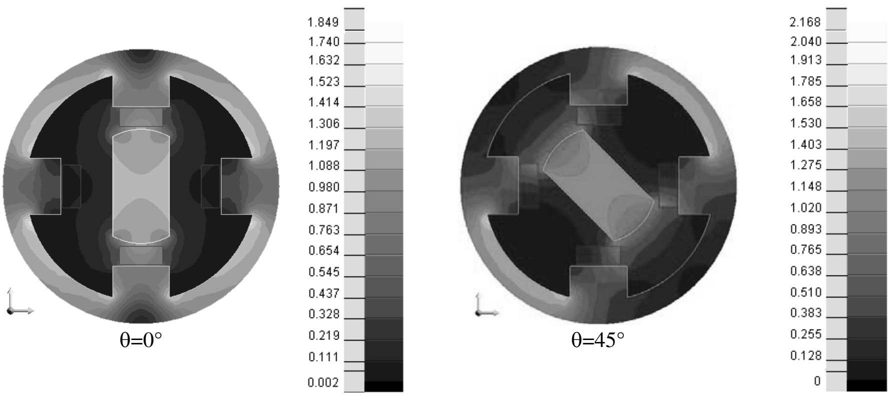

(a) Induction level distribution.

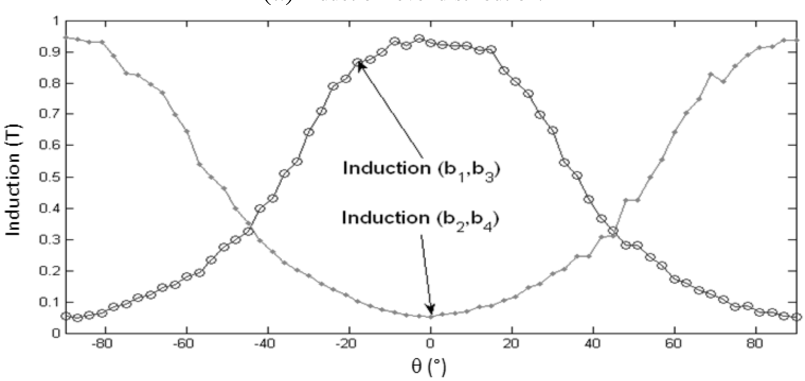

(b) Induction (T) as a function of θ (°) at the center of the beds

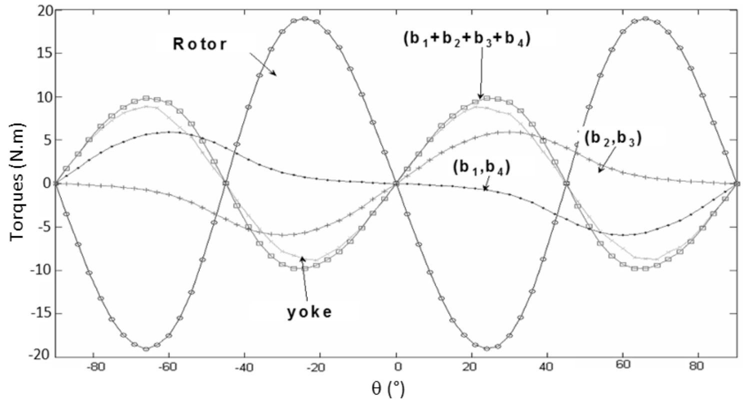

(c) Torques (N.m) as a function of θ (°)

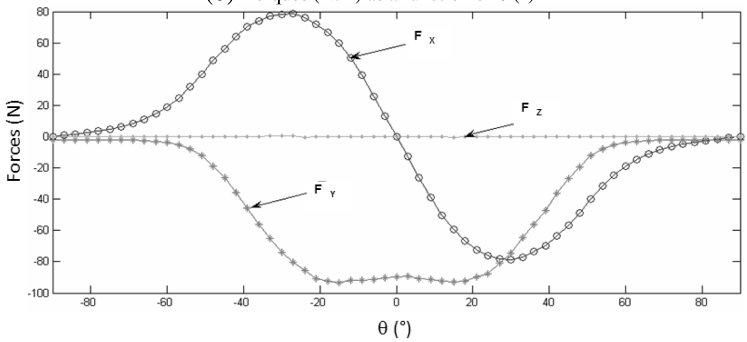

(d) Forces (N) as a function of θ (°)

Figure 4. Main results obtained on structure ⓪ (when $\theta = 0$, the magnet is along the Y axis, (b_1, b_3) are magnetized while (b_2, b_4) are demagnetized).

- Burying the beds into the yoke (Structure ⑥) is not a good solution. It allows reducing the torque but reduces in the same way the induction level and increases the forces. In practice, the flux is partially short- circuited by the yoke.
- In Structure ⑦, the inserted soft magnetic parts support a large fraction of the forces applied on the bed. Thus, X-component force is completely cancelled and the Y-component is reduced by 40%. However the induction level is also reduced because flux leakages appear between the additional parts, beds and yoke.
- Finally, a four-pole rotor (Structure ⑧) leads to an interesting configuration only for F_X reduction. The maximum induction level is lower than the one of a two-pole rotor (Structure ③). The

$B(\theta)$ variation is quasi sinusoidal with a demagnetization level of 0.1 T. Flux leakages are more important and the Y-component force is three times higher than in the Structure ③.

The main results obtained for all the configurations are given in

Table 2. Summary of the main results obtained for the nine configurations.

	Configurations		Criteria			
	N°	Geometry	$B_{\max}$ (T)	$T_{\max}$ (N.m)	$F_{X,\max}$ (N)	$F_{Y,\max}$ (N)
	⓪		0.94	19.6	78.7	93.5
	①		0.87	15.6	73.5	159.6
	②		0.9	3.6	99.4	113.7
	③		0.91	12.6	64.5	107.5
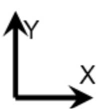	④		0.9	3.3	100.3	120
	⑤	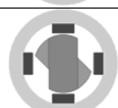	0.91	1.9	64.5	107.5
	⑥		0.72	6	122	633
	⑦	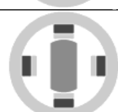	0.7	12.4	0	65.5
	⑧		0.75	3	34.3	378.5

Table 2 where $B_{\max}$, $T_{\max}$, $F_{X\max,}$ and $F_{Y\max}$ are the maximum values of the bed flux density, the total torque, the X and Y components of the force applied to beds. It allows comparison of the different configurations.

4. CONCLUSION AND PERSPECTIVES

Optimization of magnetic field sources for MR refrigeration systems should be undertaken to maximize the MCE and minimize the magnetic forces and torque. This is required to get the best performance, to insure mechanical withstanding of the refrigerant bed, a low energy consumption of the driving actuator.

In this paper, 3D finite element simulations have been performed in order to analyze the magnetic behavior of several configurations of a MR structure: smooth and salient pole yoke, 2 or 4 poles magnet, 4, 6 or 8 refrigerant beds, etc. Results show that canceling magnetic forces or torques is often achieved at the cost of the magnetic field intensity in the beds. An original structure composed of two 45° shifted half-systems is proposed and validated. Some tested configurations can be combined to obtain a better solution.

REFERENCES

1. Tishin, A. M. and Y. I. Spichkin, *Magnetocaloric Effects and Its Applications*, 475, IOP Publishing, Bristol, 2003.
2. Gschneidner, Jr., K. A., V. K. Pecharsky, and A. O. Tsokol, "Recent developments in magnetocaloric materials," *Rep. Prog. Phys.*, Vol. 68, 1479–1539, 2005.
3. Gschneidner, Jr., K. A. and V. K. Pecharsky, "Thirty years of near room temperature magnetic cooling: Where we are today and future prospects," *Int. J. Refrig.*, Vol. 31, No. 6, 945–961, 2008.
4. Nellis, G. F. and J. L. Smith, Jr., "An experimental GM/magnetic refrigerator," *Advances in Cryogenic Engineering*, Vol. 43, 1998.
5. Zimm, C., A. Jastrab, A. Sternberg, V. K. Pecharsky, K. A. Gschneider, Jr., M. Osbore, and I. Anderson, "Description and performance of near-room temperature magnetic refrigerator," *Adv. Cryog. Eng.*, Vol. 43, 1759–1766, 1998.
6. Clot, P., D. Viallet, F. Allab, A. Kedous-Lebouc, J. M. Fournier, and J. P. Yonnet, "A magnet based device for active magnetic regenerative refrigeration," *IEEE Trans. Mag.*, Vol. 39, No. 3, 3349–3351, 2003.

7. Kitanovski, A., P. W. Egolf, F. Gender, O. Sari, and C. H. Besson, "A rotary heat exchanger magnetic refrigerator," *1st International Conference on Magnetic Refrigeration at Room Temperature*, 27–30, Montreux, Switzerland, 2005.
8. Kawanami, T., K. Chiba, K. Sakurai, and M. Ikegawa, "Optimization of magnetic refrigeration at room temperature for air cooling systems," *Int. J. Refrig.*, Vol. 29, No. 8, 1294–1301, 2006.
9. Okamura, T., K. Yamada, N. Hirano, and S. Nagaya, "Performance of a room temperature rotary magnetic refrigerator," *Int. J. Refrig.*, Vol. 29, No. 6, 1327–1331, 2006.
10. Zimm, C., A. Boerder, J. Chell, A. Sternberg, A. Fujita, S. Fujieda, and K. Fukamichi, "Design and performance of a permanent-magnet rotary refrigerator," *Int. J. Refrig.*, Vol. 29, No. 6, 1302–1306, 2006.
11. Muller, C., L. Bour, and C. Vasile, "Study of the efficiency of a magnetothermal system according to the permeability of the magnetocaloric material around its curie temperature," *Second International Conference on Magnetic Refrigeration at Room Temperature*, 323, 339, Portoroz, Slovenia, 2007.
12. Lee, S. J., J. M. Kenkel, and D. C. Jiles, "Design of permanent magnet field source for rotary magnetic refrigeration systems," *IEEE Trans. Mag.*, Vol. 38, No. 2, 2991–2993, 2002.
13. Zimm, C., J. Auringer, A. Boeder, J. Chell, S. Russek, and A. Sternberg, "Design and initial performance of a magnetic refrigerator with a rotating permanent magnet," *Second International Conference on Magnetic Refrigeration at Room Temperature*, 341, 347, Portoroz, Slovenia, 2007.
14. Okamura, T., K. Yamada, N. Hirano, and S. Nagaya, "Improvement of 100W class room temperature magnetic refrigerator," *Second International Conference on Magnetic Refrigeration at Room Temperature*, 11–13, Portoroz, Slovenia, 2007.
15. Tura, A. and A. Rowe, "Design and testing of a permanent magnet refrigerator," *Second International Conference on Magnetic Refrigeration at Room Temperature*, 363–370, Portoroz, Slovenia, 2007.
16. Allab, F., "Conception et réalisation d'un dispositif de réfrigération magnétique basé sur l'effet magnétocalorique et dédié à la climatisation automobile," *Thèse de Doctorat*, Grenoble Institut National Polytechnique, 2008.
17. Zheng, Z. G., H. Y. Yu, X. C. Zhong, D. C. Zeng, and Z. W. Liu,

"Design and performance study of the active magnetic refrigerator for room-temperature application," *Int. J. Refrig.*, Vol. 32, No. 1, 78–86, 2009.

18. Cedrat Electrical Engineering, *Flux3D® Magnetostatics Tutorial*, Version 10.1, 2007.
19. Bouchekara, H., "Recherche sur les systèmes de réfrigération magnétique. Modélisation numérique, conception et optimisation," *Thèse de Doctorat*, Grenoble Institut National Polytechnique, 2008.
20. Dupuis, C., "Matériaux à effet magnétocalorique géant et systèmes de réfrigération magnétique," *Thèse de Doctorat*, Grenoble, Institut National Polytechnique de Grenoble, 2009.